

Local structure study of dilute Er in III–V semiconductors by fluorescence EXAFS

H. Ofuchi,* D. Kawamura, J. Tsuchiya, N. Matsubara, M. Tabuchi, Y. Fujiwara and Y. Takeda

Department of Materials Science and Engineering, Graduate School of Engineering, Nagoya University, Furo-Cho, Chikusa-Ku, Nagoya 464-8603, Japan.
E-mail: ofuchi@mercury.numse.nagoya-u.ac.jp

(Received 4 August 1997; accepted 1 December 1997)

For understanding the luminescence of Er atoms in III–V semiconductors, OMVPE-grown InP doped with Er has been investigated by fluorescence EXAFS (extended X-ray absorption fine structure) in order to study the local structure around Er atoms. The local structures around the Er atoms doped in InP, with doping as dilute as 3×10^{12} Er atoms in a $1.5 \text{ mm} \times 1.0 \text{ mm}$ spot, were successfully measured by fluorescence EXAFS. The EXAFS analysis revealed that the Er atoms doped in InP above 853 K (which showed low luminescence) formed the rock-salt-structure ErP, while the Er atoms doped in InP below 823 K (which showed high luminescence) substituted on the In site of InP. The dependence of the local structure on growth temperature was observed for the samples doped with 3×10^{12} atoms and 1.2×10^{13} atoms of Er.

Keywords: local structure; dilute; erbium; InP; OMVPE; EXAFS.

1. Introduction

Er-doped semiconductors have been attracting great interest because they are expected to be applied to optical communication systems (Poole *et al.*, 1992; Wang & Wessels, 1995; Takahei *et al.*, 1994; Tabuchi *et al.*, 1996). In this work, optical properties of Er doped in semiconductors were found to depend strongly on growth conditions (Fujiwara *et al.*, 1997). The difference in the luminescence intensity is considered to be related to local structures around the Er atoms which must depend on the growth temperature. Therefore, it is very important to understand the relationship between the growth conditions, the local structure around Er, and the optical properties.

In this work, we report a study of the local structure around dilute Er atoms doped in InP by EXAFS (extended X-ray absorption fine structure). EXAFS is a powerful technique for investigating local structure around a specific element (Lee *et al.*, 1981). Although the concentrations of Er atoms were as low as 3×10^{12} or 1.2×10^{13} atoms in a $1.5 \text{ mm} \times 1.0 \text{ mm}$ spot, fine structures in the EXAFS oscillation were clearly observed using a high-intensity X-ray beam and a solid-state detector (SSD) array. In this paper, ' $A \times 10^x$ atoms' means that $A \times 10^x$ atoms are contained in an X-ray irradiated area of $1.5 \text{ mm} \times 1.0 \text{ mm}$ which was fixed during the experiments, though the size can be made smaller as described later. The difference in the local structure with Er concentration is important since host semiconductors must be doped with a high concentration of Er in order to obtain high-intensity light emission. Therefore, the difference in the local structures was examined in the samples doped with 3×10^{12} and 1.2×10^{13} atoms of Er.

Table 1

Growth temperatures and Er concentrations of the samples used in this study.

Sample	Growth temperature, T_g (K)	Number of Er atoms ($\times 10^{12}$)
A	803	12
B	853	12
C	823	3
D	853	3

2. Experimental

The Er-doped InP samples were grown by a low-pressure OMVPE (organometallic vapour-phase epitaxy) on Fe-doped InP(001) substrates. Growth temperatures and Er concentrations are shown in Table 1. The Er concentrations in samples were determined by SIMS (secondary-ion mass spectroscopy). The thicknesses of the grown layers were about $1 \mu\text{m}$ for all samples. Details of the growth process and characterization technique for Er-doped InP have been described elsewhere (Fujiwara *et al.*, 1995).

The EXAFS measurements were conducted using synchrotron radiation at beamline BL12C of the Photon Factory in the National Laboratory for High Energy Physics at Tsukuba. The X-ray beam was monochromated by an Si(111) double-crystal monochromator and focused by an Rh-coated bent cylindrical mirror. Using these optics, the X-ray spot size was made less than $1 \text{ mm} \times 0.5 \text{ mm}$ and the photon flux was about $10^{10} \text{ mm}^{-2} \text{ s}^{-1}$. During the EXAFS measurement and wavelength scan the spot size and position were very stable. The EXAFS spectra were measured at the Er L_{III} -edge in the fluorescence-detection mode. The incident X-ray beam intensity was monitored by a nitrogen-filled ionization chamber, while the fluorescence X-ray signal was detected by a 19-channel Ge SSD. Using the high-intensity X-ray

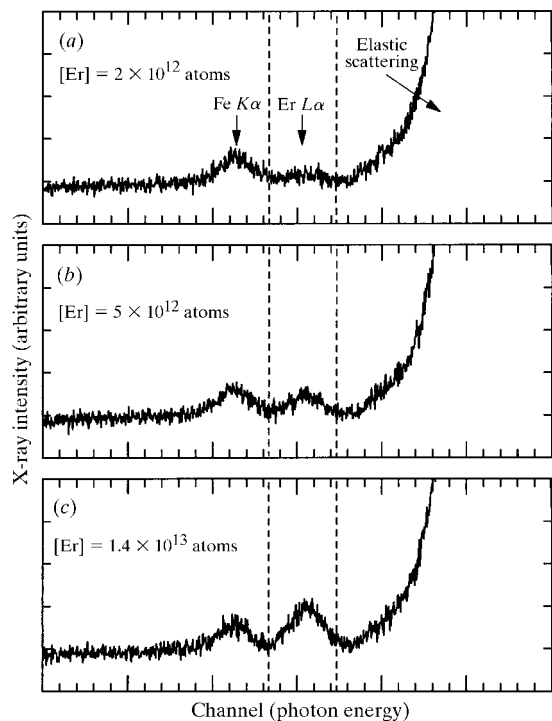


Figure 1

X-ray energy spectra of samples with (a) $[\text{Er}] = 2 \times 10^{12}$ atoms (the number of Er atoms in a $1.5 \text{ mm} \times 1.0 \text{ mm}$ spot), (b) $[\text{Er}] = 5 \times 10^{12}$ atoms, and (c) $[\text{Er}] = 1.4 \times 10^{13}$ atoms.

beam and the 19-channel SSD, the measurement for the samples with such a dilute Er could be conducted within 1 d for one sample, even for the lowest Er density. All the measurements were performed at room temperature.

Fig. 1 shows fluorescence X-ray energy spectra for Er-doped InP. The energies of Er $L\alpha$ and Fe $K\alpha$ X-rays are indicated by arrows in Fig. 1. The Fe $K\alpha$ X-rays are due to Fe contained as impurities in the InP substrate and/or the measurement system. For the samples doped with 1.4×10^{13} atoms of Er, a peak of Er $L\alpha$ was clearly observed. However, for the sample doped with 2×10^{12} atoms of Er, it is difficult to find a peak for Er $L\alpha$. The X-ray intensity integrated between two broken lines shown in Fig. 1 was defined as the fluorescence intensity of Er. Fig. 2 represents the EXAFS oscillations for the samples shown in Fig. 1. Corresponding to the results shown in Fig. 1, the spectra of the samples doped with 1.4×10^{13} atoms and 5×10^{12} atoms of Er were relatively clear; however, that of the sample doped with 2×10^{12} atoms of Er was noisy. Therefore, it is considered that an Er concentration between 2×10^{12} atoms and 5×10^{12} atoms is a limit to this measurement system at present.

3. Results and discussions

Fig. 3 represents the Fourier transformed EXAFS oscillations for all the samples. For the samples doped with 1.2×10^{13} atoms of Er, high-quality spectra were obtained as shown in Fig. 3(a). For the samples grown below 823 K, a main peak due to the first coordination shell around Er was observed at 2.2 Å. On the other hand, for the samples grown above 853 K, the main peak shifted towards a longer radial distance compared with the samples grown below 823 K.

In order to analyse the details of the measured spectra, curve fitting was performed in the range 2.6–10.3 Å⁻¹ using theoretically calculated spectra (FEFF6; Rehr *et al.*, 1991). The fitting parameters for the best fit for the samples doped with 1.2×10^{13} atoms of Er are listed in Table 2. Bond length, r , coordination number, N , and Debye–Waller factor, σ , were chosen as the fitting parameters.

In the sample grown at 803 K, the Er–P bond length was found to be 2.67 ± 0.02 Å, which is close to the sum of Er and P covalent radii ($1.57 + 1.10 = 2.67$ Å). In the sample grown at 853 K, on the other hand, the Er–P bond length was found to be 2.77 ± 0.03 Å.

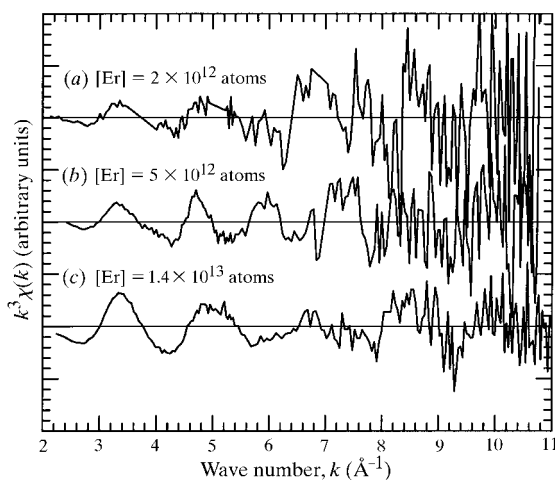


Figure 2 EXAFS oscillations for samples as shown in Fig. 1 with (a) $[\text{Er}] = 2 \times 10^{12}$ atoms, (b) $[\text{Er}] = 5 \times 10^{12}$ atoms, and (c) $[\text{Er}] = 1.4 \times 10^{13}$ atoms.

Table 2

Results of the curve fitting.

r , bond length; N , coordination number; σ , Debye–Waller factor. The errors of the R values are $\Delta r = \pm 0.03$ Å and the errors of the coordination numbers and Debye–Waller factors are 20–30%.

Sample	r (Å)	N	σ (Å)
A	2.67	3.9	0.11
B	2.77	7.3	0.11

The bond length was close to 2.803 Å, which is the known Er–P bond length in the NaCl-structure ErP (Guivarc’h *et al.*, 1989). The coordination numbers obtained from the curve fitting for the samples grown at 803 and 853 K were 3.9 and 7.3, respectively. These coordination numbers are close to 4 for the zinc-blende structure and 6 for the rock-salt structure. For the samples doped with 3×10^{12} atoms of Er, judging from Fig. 3, it is likely that they will have the same parameters as the samples doped with 1.2×10^{13} atoms of Er. A detailed analysis of these samples will be described in a forthcoming paper (Ofuchi *et al.*, 1998).

4. Conclusions

For understanding the luminescence properties of the Er atoms in III–V semiconductors, we have investigated OMVPE-grown InP doped with Er by fluorescence EXAFS in order to study local structures around the Er atoms. The local structures around the Er atoms doped in InP, with doping as dilute as 3×10^{12} Er atoms, were successfully measured by fluorescence EXAFS. The EXAFS analysis revealed that the Er atoms doped in InP above 853 K (which showed low luminescence) formed the rock-salt-structure ErP, while the Er atoms doped in InP below 823 K (which showed high luminescence) are substituted on the In site of InP. A similar dependence of the local structure on growth temperature was

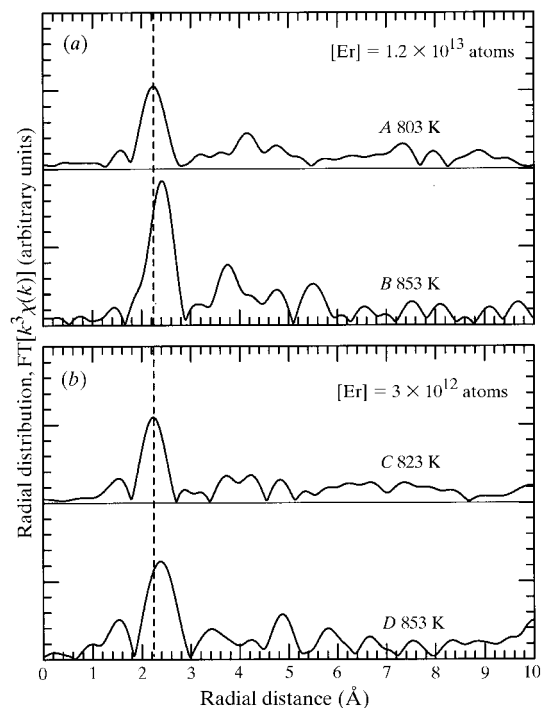


Figure 3 Fourier transforms of $k^3\chi(k)$ between $k = 2.4$ and 10.5 Å⁻¹. (a) $[\text{Er}] = 1.2 \times 10^{13}$ atoms grown at 803 K (A) and at 853 K (B), and (b) $[\text{Er}] = 3 \times 10^{12}$ atoms grown at 823 K (C) and at 853 K (D).

observed for the samples doped with 3×10^{12} atoms and 1.2×10^{13} atoms of Er.

This work was performed as part of the project (Project No. 95 G221) accepted by the Photon Factory Program Advisory Committee, and was supported in part by the Grant-in-Aid for Developmental Scientific Research (A)(1) No. 7555100 and (A)(2) No. 09305330 and for Science Research of Priority Area, Spin-Controlled Semiconductor Nanostructure No. 09244209 from the Ministry of Education, Science and Culture.

References

- Fujiwara, Y., Furuta, S., Makita, K., Ito, Y., Nonogaki, Y. & Takeda, Y. (1995). *J. Cryst. Growth*, **146**, 544–548.
- Fujiwara, Y., Matsubara, N., Tsuchiya, J., Ito, T. & Takeda, Y. (1997). *Jpn. J. Appl. Phys.* **36**, 2587–2591.
- Guivarc'h, A., Caulet, J. & Le Corre, A. (1989). *Electron. Lett.* **25**, 1050–1052.
- Lee, P. A., Citrin, P. H., Eisenberger, P. & Kincaid, B. M. (1981). *Rev. Mod. Phys.* **53**, 769–806.
- Ofuchi, H., Kawamura, D., Matsubara, N., Tabuchi, M., Fujiwara, Y. & Takeda, Y. (1998). *Microelectron. Eng.* In the press.
- Poole, I., Singer, K. E., Peaker, A. R. & Wright, A. C. (1992). *J. Cryst. Growth*, **121**, 121–131.
- Rehr, J. J., Mustre de Leon, J., Zabinsky, S. I. & Albers, R. C. (1991). *J. Am. Chem. Soc.* **113**, 5135–5140.
- Tabuchi, M., Kawamura, D., Fujita, K., Matsubara, N., Ofuchi, H., Ichiki, S., Kamei, H. & Takeda, Y. (1996). *Mater. Res. Soc. Symp. Proc.* **422**, 155–160.
- Takahei, K., Taguchi, A., Horikoshi, Y. & Nakata, J. (1994). *J. Appl. Phys.* **76**, 4332–4339.
- Wang, X. Z. & Wessels, B. W. (1995). *Appl. Phys. Lett.* **67**, 518–520.